CHAPTER 4

BENDER ELEMENT TESTS

4.1 General

The impact of hydrocarbon on various geotechnical properties of diversified soils have been reported in the literature. Nevertheless, shear wave velocity (V_s) of hydrocarbon-contaminated soils has not been precisely focused. Several studies have been conducted to evaluate the behavior of hydrocarbon contaminated soil. It is worth mentioning that hydrocarbon contamination may also induce microstructural changes in soil which may directly affect its response at the macroscale. One such response is propagation of shear waves through the soil matrix. Shear wave velocity is a vital parameter in studying soil-structure interaction effects (Siang et al. 2014) and liquefaction analysis (Yunmin et al. 2005; Zhou and Chen 2007). Several empirical charts have been developed to correlate shear wave velocity with the liquefaction potential of soils in the field (Robertson and Ferreira 1992; Addo and Robertson 1992; Kayen et al. 2013; Andrus and Stokoe II 2000; Tokimatsu and Uchida 1990). The laboratory measured shear wave velocities have also been correlated with the cyclic resistance ratio after making some adjustments for the field conditions (Simatupang et al. 2018). Moreover, it should be stated that the determination of shear wave velocity in very small strain conditions is significant due to this fact that soil maximum shear modulus (G_{max} or G_0) can be calculated using $G_{max} = \rho V_s^2$, where ρ = density of soil. It is obvious from the reported literature that there has not been much focused study on the influence on hydrocarbon contamination on the shear wave velocity and small-strain shear modulus as an influential parameter in small/very small strain problems such as design of machine foundations, ground response analysis (Castelli et al. 2018; Cavallaro et al. 2013). Some resistivity based methods have been documented in the past to assess the spatial distribution of the hydrocarbons in the subsoil (Arrubarrena-Moreno & Arango-Galván,

2013; Abdullah et al. 2014). Also, mechanical properties of the oil contaminated soil have also been evaluated using resistivity techniques by Bian et al. (2018). Analogously, being a non-destructive field test, such a study using Bender element would aid in the evaluation of subsoil responses for both undeveloped as well as developed sites. It may also help to identify the severity as well as extent of contamination before implementing suitable remediation techniques. Only a few studies (Rajabi and Sharifipour 2017a; Rajabi and Sharifipour 2017b) have been taken up in this context leaving behind a vast scope for a parametric study.

This chapter deals with investigating the effect of crude oil contamination on shear wave velocity of sandy samples by performing a series of bender element tests under various excitation frequencies, confining pressure and contamination depth. The main focus is to elucidate the effect of hydrocarbon contamination on the shear wave velocity of Guwahati sand which can later be used to assess the liquefaction propensity as per the available correlations.

4.2 Description of Experimental Setup

4.2.1 Test Combinations and Selection of Parameters

Based on five different parameters, a total of 150 test combinations were analyzed in the current study. Table 4.1 depicts the range of each of the five variables considered, while Table 4.2 shows the summary of various test combinations.

Table. 4.1 Variables along with their considered range

Parameter	Range
Frequency	Ranging from 1 kHz to 10 kHz with step increment of 1kHz
Confining Pressure (σ_c)	100 kPa, 150 kPa and 200 kPa
Crude oil content (ω)	0-12% with step increment of 2%
Contamination Depth Ratio (β)	0, 0.356, 0.55, 0.75, 1
Saturation	Dry condition and Fully saturated condition

Range of frequency has been selected on the basis of past experimental works which has been correlated with the field investigations. The frequency usually lies in the range of several tenths to several Hz in quasi-static loading tests and several tens Hz in RC tests, but several to a few tens kHz in BE tests (Gu et al. 2015).

Table. 4.2 Summary of bender element testing series in the present study

Sample Type	**Dry Condition (σ_c, ω)**				**Fully saturated condition (σ_c, ω)**			
Homogeneous	(100,0)	(150,0)	(200,0)	(100,2)	(100,0)	(150,0)	(200,0)	(100,2)
	(150,2)	(200,2)	(100,4)	(150,4)	(150,2)	(200,2)	(100,4)	(150,4)
	(200,4)	(100,6)	(150,6)	(200,6)	(200,4)	(100,6)	(150,6)	(200,6)
	(100,8)	(150,8)	(200,8)	(100,10)	(100,8)	(150,8)	(200,8)	(100,10)
	(150,10)	(200,10)	(100,12)	(150,12)	(150,10)	(200,10)	(100,12)	(150,12)
	(200,12)				(200,12)			
	Dry Condition (σ_c, ω, β)				**Fully saturated condition (σ_c, ω, β)**			
Layered	(100,2,0.356)	(150,2,0.356)	(150,2,0.356)		(100,2,0.356)	(150,2,0.356)	(150,2,0.356)	
	(100,2,0.55)	(150,2,0.55)	(200,2,0.55)		(100,2,0.55)	(150,2,0.55)	(200,2,0.55)	
	(100,2,0.75)	(150,2,0.75)	(200,2,0.75)		(100,2,0.75)	(150,2,0.75)	(200,2,0.75)	
	(100,4,0.356)	(150,4,0.356)	(200,4,0.356)		(100,4,0.356)	(150,4,0.356)	(200,4,0.356)	
	(100,4,0.55)	(150,4,0.55)	(200,4,0.55)		(100,4,0.55)	(150,4,0.55)	(200,4,0.55)	
	(100,4,0.75)	(150,4,0.75)	(200,4,0.75)		(100,4,0.75)	(150,4,0.75)	(200,4,0.75)	
	(100,6,0.356)	(150,6,0.356)	(200,6,0.356)		(100,6,0.356)	(150,6,0.356)	(200,6,0.356)	
	(100,6,0.55)	150,6,0.55)	(200,6,0.55)		(100,6,0.55)	150,6,0.55)	(200,6,0.55)	
	(100,6,0.75)	(150,6,0.75)	(200,6,0.75)		(100,6,0.75)	(150,6,0.75)	(200,6,0.75)	
	(100,8,0.356)	(150,8,0.356)	(200,8,0.356)		(100,8,0.356)	(150,8,0.356)	(200,8,0.356)	
	(100,8,0.55)	(150,8,0.55)	(200,8,0.55)		(100,8,0.55)	(150,8,0.55)	(200,8,0.55)	
	(100,8,0.75)	(150,8,0.75)	(200,8,0.75)		(100,8,0.75)	(150,8,0.75)	(200,8,0.75)	
	(100,10,0.356)	(150,10,0.356)	(200,10,0.356)		(100,10,0.356)	(150,10,0.356)	(200,10,0.356)	
	(100,10,0.55)	(150,10,0.55)	(200,10,0.55)		(100,10,0.55)	(150,10,0.55)	(200,10,0.55)	
	(100,10,0.75)	(150,10,0.75)	(200,10,0.75)		(100,10,0.75)	(150,10,0.75)	(200,10,0.75)	
	(100,10,0.356)	(150,12,0.356)	(200,12,0.356)		(100,10,0.356)	(150,12,0.356)	(200,12,0.356)	
	(100,12,0.55)	(150,12,0.55)	(200,12,0.55)		(100,12,0.55)	(150,12,0.55)	(200,12,0.55)	
	(100,12,0.75)	(150,12,0.75)	(200,12,0.75)		(100,12,0.75)	(150,12,0.75)	(200,12,0.75)	

4.2.2 Instrumentation Details

Bender element apparatus was employed in the present study to obtain the shear wave velocity of the sand specimens. The block diagram of the test set up is shown in Fig. 4.1. A pair of piezo-ceramic bender elements (transmitter-receiver pair) are provided at each end of the soil sample. The function generator generates a sine wave of frequency ranging from 1-10 kHz and amplitude 20 V peak to peak which was used to excite the transmitter. The transmitted wave was received at the other end by a receiver which was connected to a digital oscilloscope equipped with a filter and amplifier. The digital oscilloscope also receives sine wave from function generator and displays both input and output signal waves.

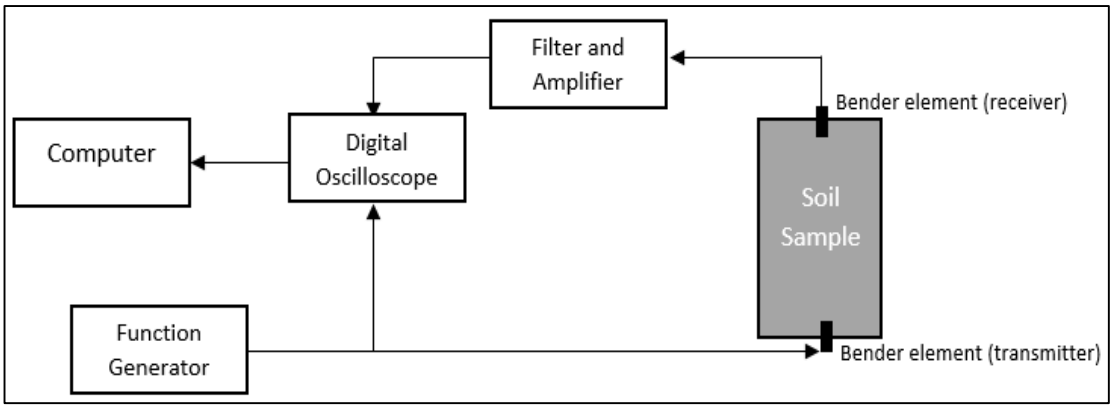

Fig. 4.1 Schematic depicting working of bender element test set-up

The time lag between the input and output waves can be determined by adjusting the cursor positions in the oscilloscope display which directly gives the travel time of the shear wave along the sample length. Consequently, by knowing that the distance of travel i.e. the tip-to-tip distance between the two elements, the speed of the shear wave, V_s, can be determined as

$$V_s = \frac{L_{TT}}{\Delta t} \tag{4.1}$$

where, L_{TT} is the wave travel distance (tip-to-tip distance between the source and the receiving elements), and Δt is the wave travel time.

4.2.3 Sample Preparation and Test Procedure

Both dry and quasi-moist tamping methods were employed for preparing the clean (uncontaminated) and contaminated samples respectively. Quasi-moist tamping method for preparation of contaminated samples involved mixing of the oven-dried sand with calculated amount of crude oil after which the moist sand was deposited into a cylindrical split mold (dia 50mm) and compacted in 5 layers. Each layer was compacted using a small tamper. The number of blows applied for each layer was carefully controlled. In order to achieve sample uniformity and desired relative density (D_r) of approximately 50% (Rajabi and Sharifipour 2017b), under-compaction technique proposed by Ladd (1978) was employed. For each layer, the compactive effort was increased towards the top with the under compaction ratio of 2.5 %. Additionally, a suction of 20kPa was employed to hold the sample vertically. After attaining the desired height (10cm) and void ratio, the top bender element was carefully assembled with a proper O-ring head. The two way split sampling mold was released and the perspex cell was carefully placed and tightly connected to the base pedestal to provide well-fitted condition for applying isotropic confining pressure. In the testing procedure, the specimens were subjected to confining pressures of 100, 150 and 200 kPa. Fig 4.2(a)-(e) shows the schematic of step by step procedure of the sample preparation.

The study of the effect of depth of the contaminated layer has been incorporated in terms of L_c/L ratio (referred as contamination depth ratio, β hereafter) where L_c is the depth of the contaminated layer and L is the total length of the sample. In this regard, β with a value of 0, 0.35, 0.55, 0.75 and 1 was considered as shown in Fig. 4.3. Here, $\beta = 0$ represents the

clean sand samples while β = 1 represents homogeneously contaminated samples. The procedure for preparation of such a layered sample is same as that of homogeneous samples. All the prepared specimens were tested under both dry and saturated conditions.

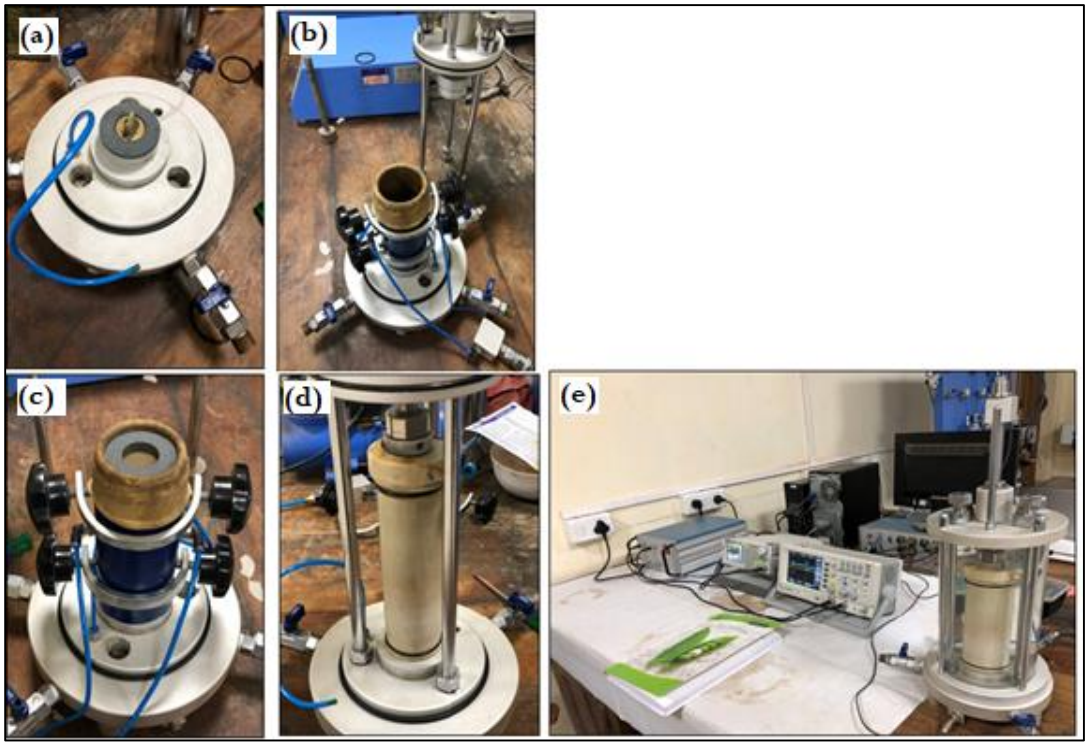

Fig. 4.2 Steps involved in sample preparation and assembly in bender element testing

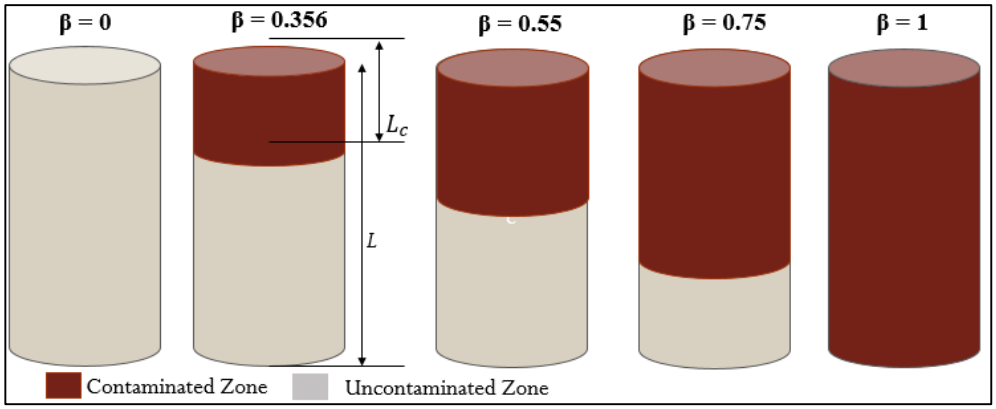

Fig. 4.3 Schematic representation of samples for evaluation of depth of hydrocarbon contamination

4.3 Signal Interpretation

The most challenging aspect of a Bender Element Test is interpreting the data, or correctly determining the shear wave's travel time. The shear wave is difficult to discern in most situations because the emitted signal includes noise and/or is distorted by the arrival of other forms of waves. As a result, several methods for interpreting the Bender Element test have been developed. The two popular approaches, Peak-to-Peak and Start-to-Start, has been considered in this study. Other methods can be found in the literature and have not been covered here. The transmitted and received signals must be synchronized, by the oscilloscope, and presented on a single plot so that they can be analyzed. The time difference between those two will define the transit time of the shear wave (Fig. 4.4). The received signal might not be as clear as transmitted signal and so it is important that one should make a judgement about what method of interpretation must be used.

4.3.1 Peak-to-Peak Method

In this method, the time of travel is defined as the time between the peak of the transmitted signal and the first peak of the received signal (Fig. 4.5). This method is the most common one, as it ignores the first arrival of the shear wave which can be due to the near-field effect.

4.3.2 Start-to-Start Method

In this method, the time of travel is defined as the time between the start of the transmitted signal and the start of the received signal (Fig. 4.6). This method might produce better results as the near-field effect is not affecting the waveform.

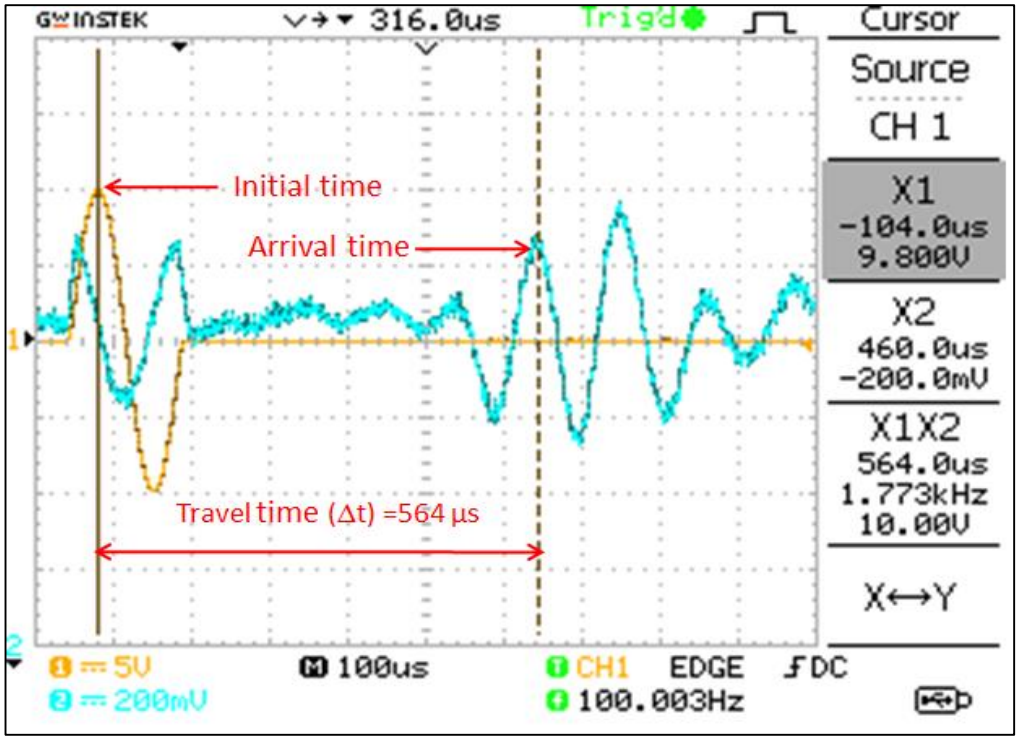

Fig. 4.4 Typical oscilloscope screen showing input and output signals

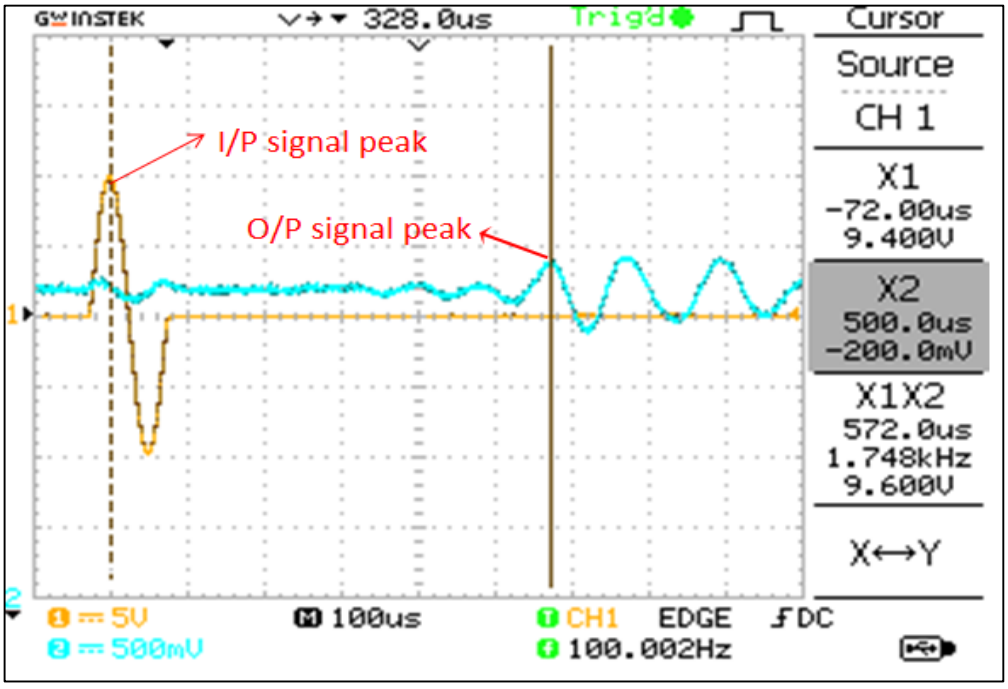

Fig. 4.5 Typical oscilloscope screen indicating peaks of input and output signals

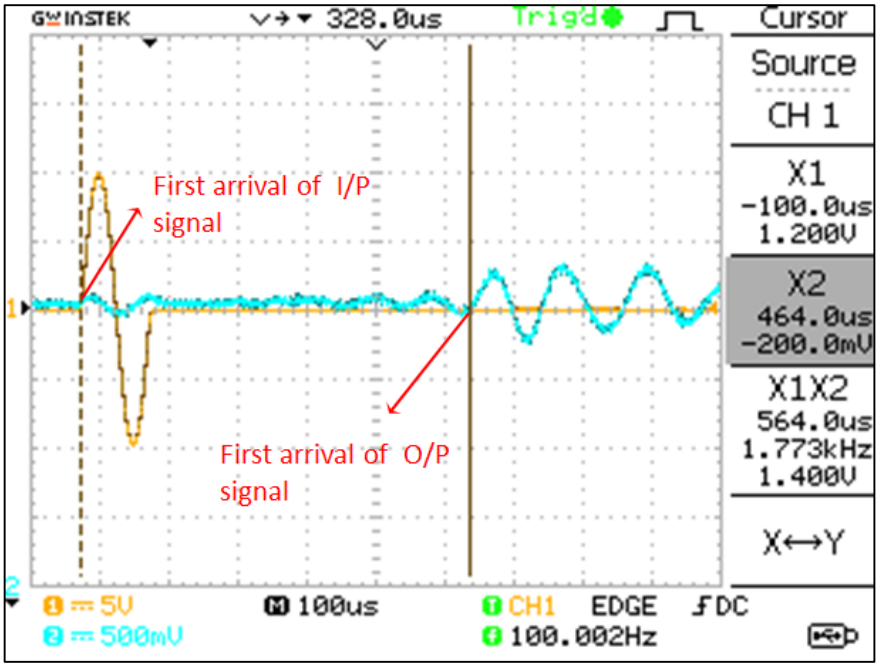

Fig. 4.6 Typical oscilloscope screen indicating arrival/start of input and output signals

4.3.3 Boundary effects

The selection of method to determine shear wave velocity among various temporal methods such as peak-to-peak, start-to-start and mathematical methods such as cross-correlation is an important concern. After profoundly concentrating on the previous literature (Rajabi and Sharifipour 2017b) peak-to-peak method was adopted to determine the shear wave travel time hereafter in this study. Additionally, a transmitted shear wave is typically accompanied by a boundary induced compression wave, which can often mask the shear wave at the receiver end, making precise travel time determination difficult. This effect was termed as near field effect (NFE) in the literature (Arroyo et al. 2006; Brignoli et al. 1996). However, since the near field effect induced by the boundary in the received signal is a dispersive (frequency dependent) phenomenon, it can be anticipated that the influence of NFE can be altered by changing frequency (Yamashita et al. 2009). In order to lessen the influences of

NFE a practical guideline was proposed by Jovicic et al. (1996) in terms of R_d which denotes the number of wavelengths occurred between the bender elements and is expressed as

$$R_d = \frac{L}{\lambda} \tag{4.2}$$

where, L= distance between transmitter and receiver

λ = wavelength of input signal

It has been stated that the NFE was prominent for the value of R_d between 0.24 and 4. For higher values of R_d (≥ 4), the influences of NFE were greatly alleviated. In addition, to weaken the effects of near effects, Leong et al. (2009), also suggested that it would be better to design configuration of Bender element test with the amount of R_d greater than 3.33. In the present study, all the frequencies within the proposed consistency range exceeds the suggested critical value for R_d and hence the boundary effects were not significant.

4.4 Results Interpretation and Discussion

4.4.1 Effect of Excitation Frequency

The transmitted and received shear wave signal for the bender element tests on clean Guwahati sand with σ_c = 200 kPa and D_r = 50% under various frequencies ranging from 1-10 kHz have been provided in Fig. 4.7. The frequency ranges of 1-10 kHz was selected to evaluate the influence of excitation frequency on shear wave velocity of sand and to find the "consistency range" of frequencies at which most accurate results can be obtained. It is evident from the figure that with increasing frequency, the peak of the received signal tends

to move towards left indicating reduced travel time and hence increased shear wave velocity. For higher frequencies (≥ 8kHz), the peaks of the received signals were placed almost at the similar positions while for lower frequency range (< 8 kHz), the arrival of the peaks were different.

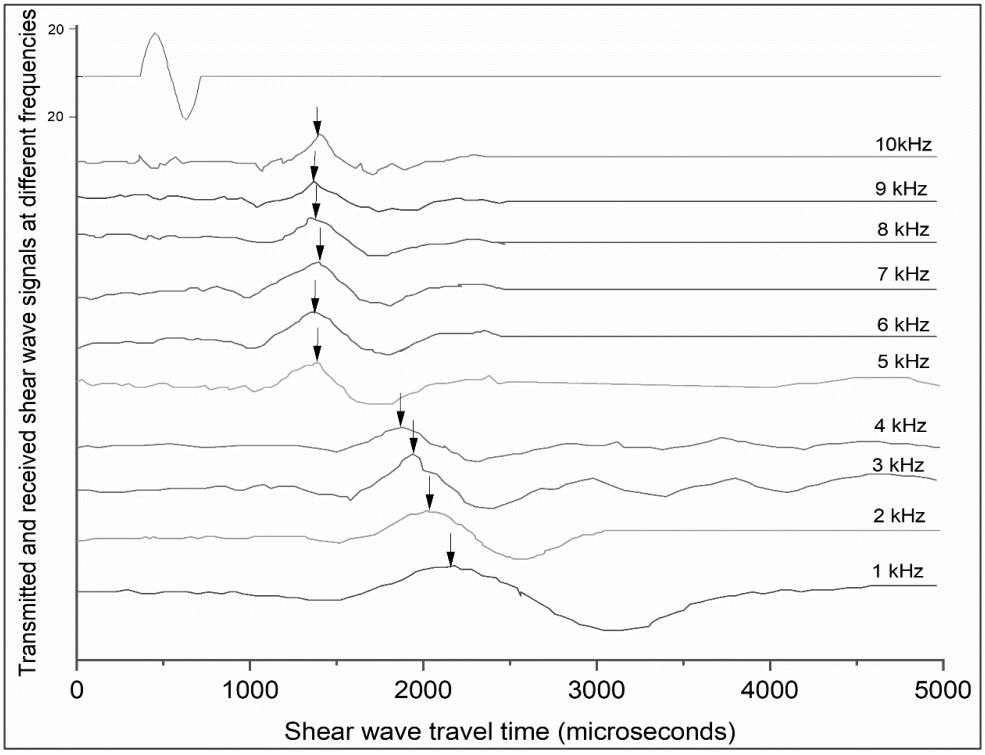

Fig. 4.7 Bender element test results on clean oven-dried Guwahati sand with σ_c=200kPa at various excitation frequencies

Fig. 4.8 depicts the bender element test results for clean as well as contaminated sand specimens under varying excitation frequencies (1-10 kHz) at different confining pressures (100, 150 and 200kPa) for dry samples. Ignoring slight scattering at lower frequency, there is not much significant change in the shear wave velocity for frequency ≥ 8 kHz. Analogous observations were made for saturated samples which have been shown in Fig. 4.9. Hence, in regard with the present study 8-10 kHz can be considered as the consistency range of frequency for given soil conditions.

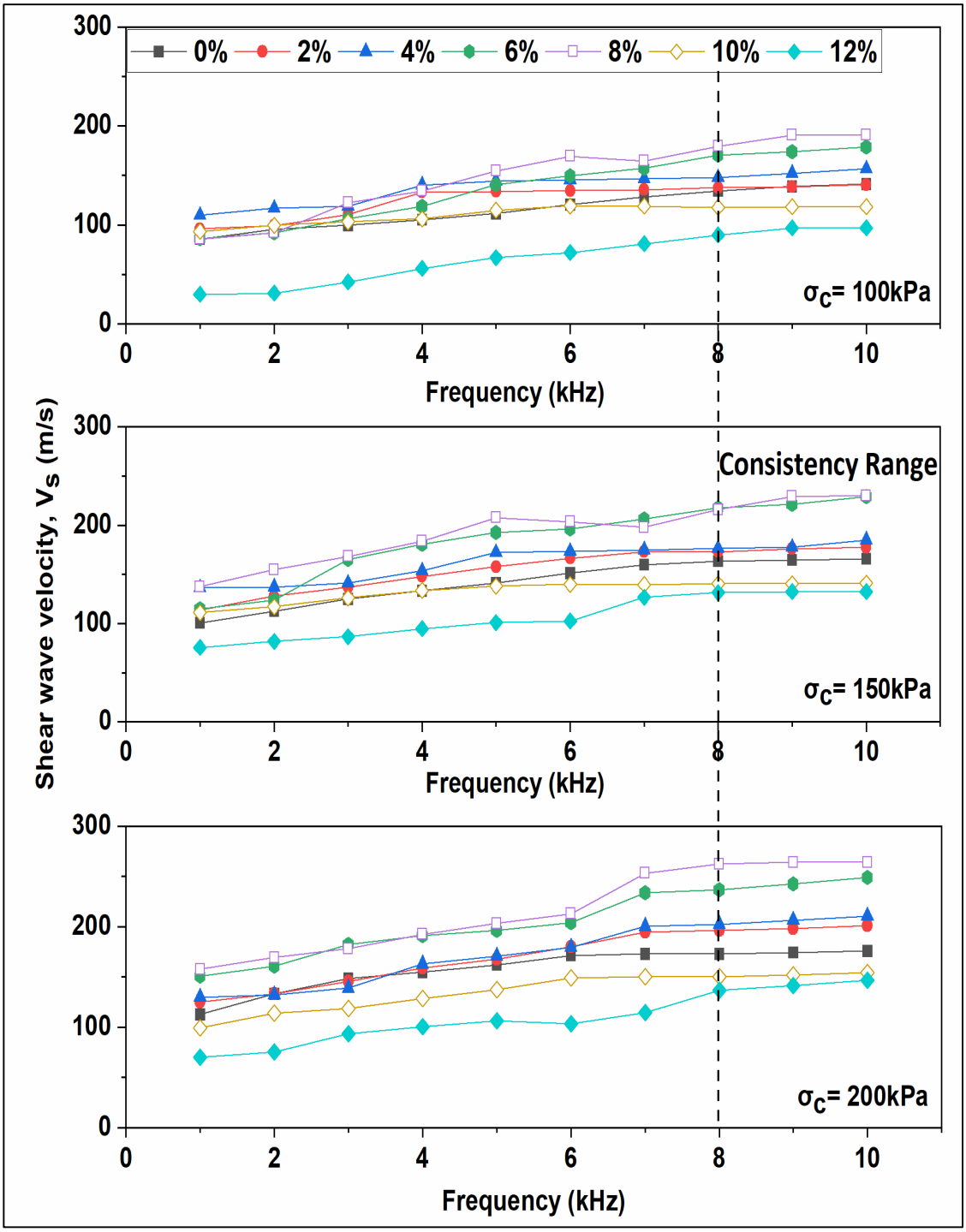

Fig. 4.8 Effect of excitation frequency on shear wave velocities of uncontaminated and contaminated dry sand specimens

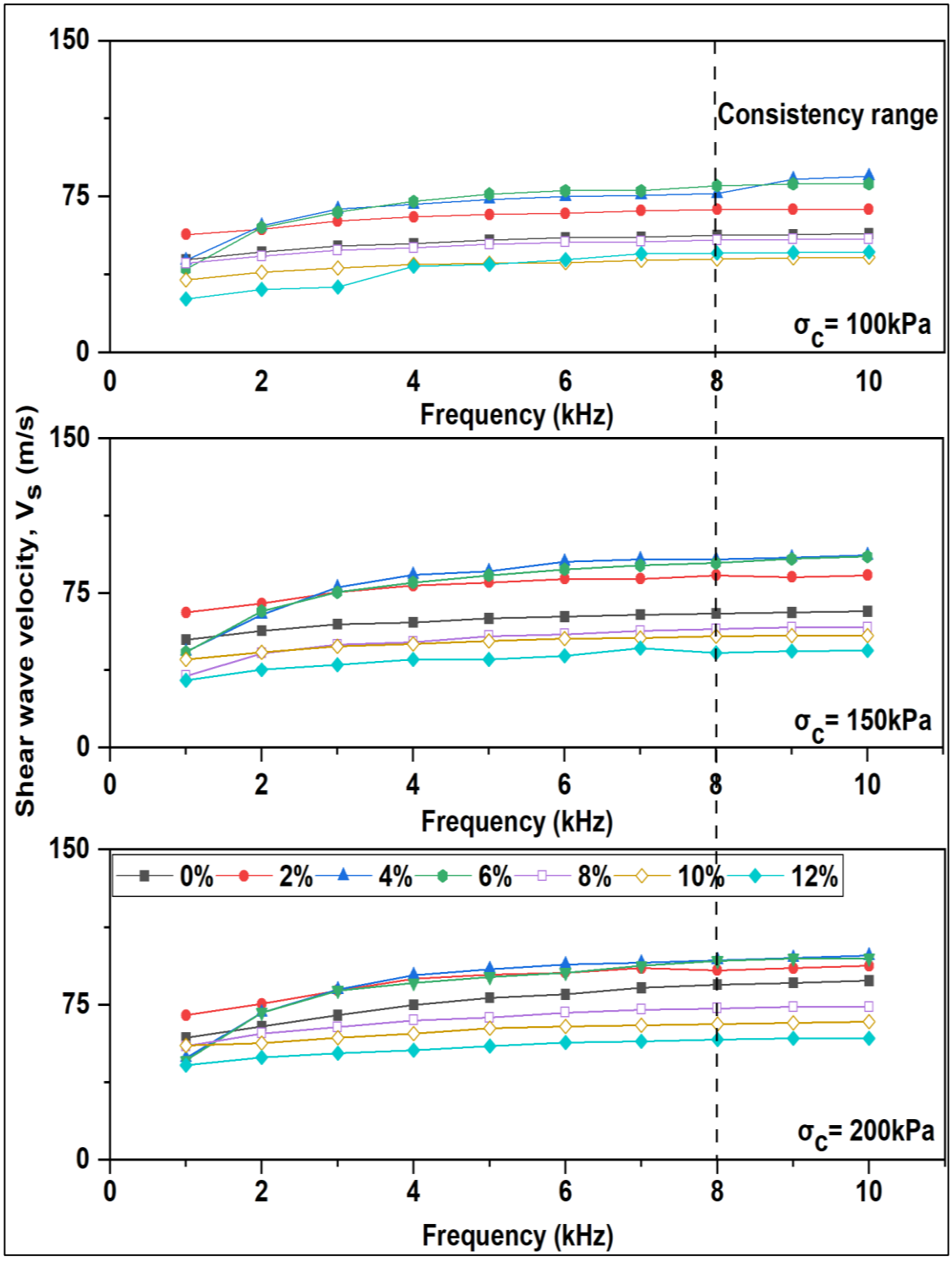

Fig. 4.9 Effect of excitation frequency on shear wave velocities of uncontaminated and contaminated saturated sand specimens

4.4.2 Effect of Crude Oil Content on Homogeneously Contaminated Samples

The influence of crude oil contamination on shear wave velocity of Guwahati sand is depicted in Fig. 4.10. The test was conducted for varying oil dosages (2, 4, 6, 8, 10 and 12%) at 3 different confining pressures of 100, 150 and 200 kPa in dry as well as saturated state.

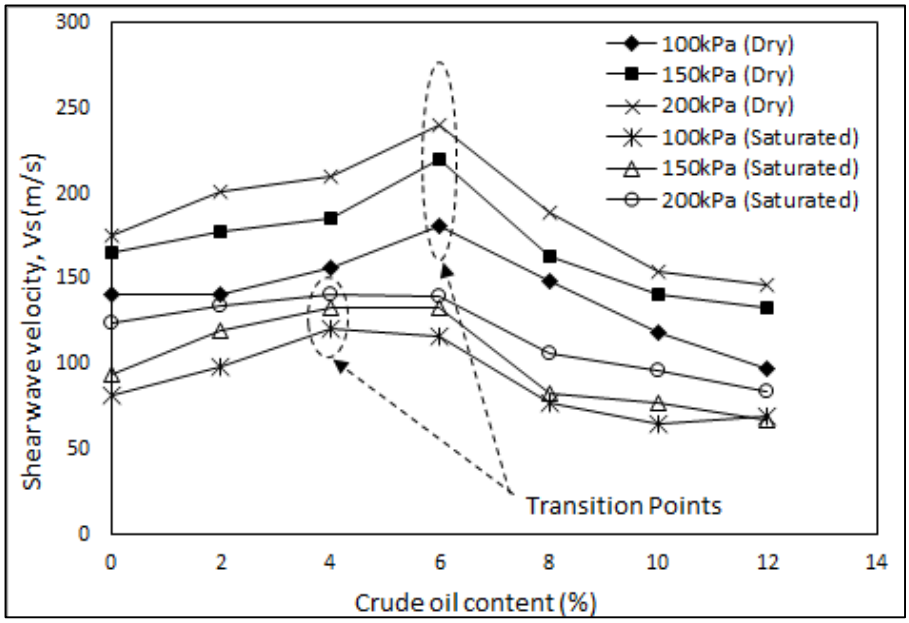

Fig. 4.10 Variation of shear wave velocity with crude oil content at different confining pressures

From the figure, it was observed that crude oil contamination markedly affects the shear wave velocity profiles. Initially adding crude oil into the sand significantly increases the shear wave velocity and S-wave velocity profile of dry samples observes its peak at 6%. Likewise, the peaks of the S-wave velocity profile of saturated samples shifts from 6% to 4% with an apparent dip compared to the dry samples. The trend was same for all confining pressures. This observation can be associated with the previous studies related to saturation-capillary pressure studies (Mako 2005) which states that as the amount of non-polar/non-aqueous phase liquid in the soil increases, the capillary induced pressure remarkably

decreases. However, adding further crude oil has brought a substantial negative impact and a sudden dip in the shear wave velocity was observed for oil content greater than 6% and 4% for dry and saturated specimens respectively. These oil content can be regarded as critical oil contents and the points corresponding to these oil contents in the shear wave velocity profiles are marked as "transition points" from where transition in the trend of shear wave velocity profiles can be observed. This behavior of shear wave velocity profiles due to crude oil contamination can be explained through microstructural investigations shown in Fig. 3.13. It is evident from the figures, for lower oil contents i.e. up to 8%, oil occupies the inter-granular voids in the form of oil droplets resulting into a more connected soil skeleton to facilitate the propagation of shear wave through it. There is also development of hydrocarbon-induced cohesion which further helps in maintaining grain to grain contact for shear wave propagation. However, the amount of crude oil was not sufficient to completely coat the sand grains and bring any significant changes in surface roughness and interlocking of sand grains. Adding crude oil beyond 8% brought noticeable changes in the soil skeleton. The inter-granular spaces were completely filled with the oil. Additionally, the sand grains get completely smeared with crude oil layer and the inter-particle contact friction almost vanish.

4.4.3 Effect of Confinement

The variation in confining pressures brings about substantial alterations in the shear wave velocity of both clean and contaminated sand. It is evident from Fig. 4.11, the shear wave velocity increased with increasing the confining pressure for all percentages of crude oil for both dry and saturated states. The confinement-induced changes in shear wave velocity of contaminated sand is slightly diminished at higher confining pressures (Fig. 4.11b).

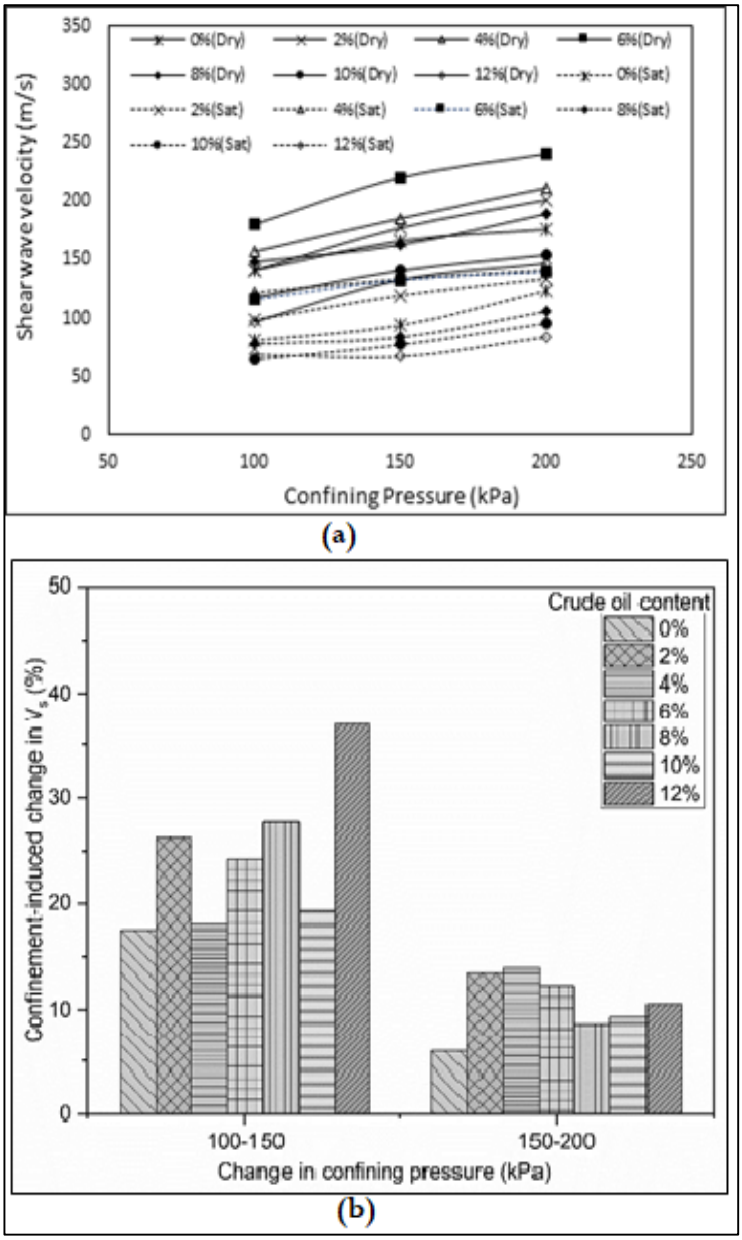

Fig. 4.11(a) Shear wave velocity of clean and contaminated Guwahati sand under different confining pressures (b) Confinement induced change in shear wave velocity of clean and contaminated Guwahati sand

This observation can be attributed to the fact that at lower confining stresses the possibility of sand particles to move into the soil voids and attain a more compacted skeleton is more. But with increasing confining stresses this possibility gradually weakens. In addition, in case of sand contaminated with higher percentages of crude oil, there is a likelihood of oil

occupying the pore spaces and thus restricting the sand grains to move closer. Therefore, confinement induced changes are even more diminished at higher oil contents.

The percentage change in the shear wave velocities owing to oil contamination at different confining pressures has been depicted in the Fig. 4.12. For each case, the change has been calculated with respect to the clean sand. Positive values indicate the increase in shear wave velocity and vice versa. For dry samples, there is an increase in percentage change with increasing oil content irrespective of the nature of the change. The observed behavior was same for all confining pressures. However, no specific trend was observed for percentage change of shear wave velocity in oil contaminated saturated samples as for saturated samples there was a combined effect of water and oil as pore fluids.

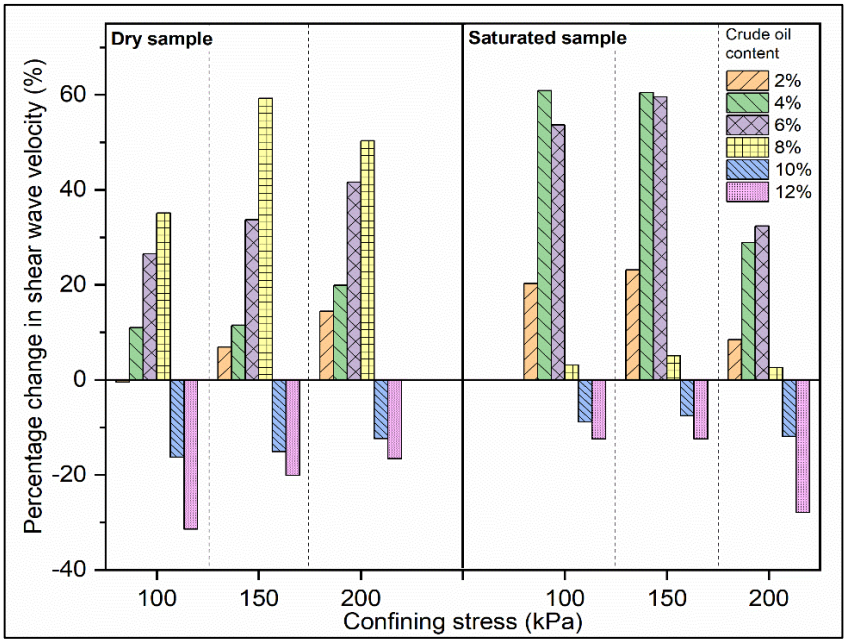

Fig. 4.12 Comparative chart for percentage change in shear wave velocity of clean and contaminated Guwahati sand under different confining stresses and saturation condition

4.4.4 Comparison with Past Reported Results

The geotechnical properties of the Guwahati sand were compared (Table 4.3) with that of Ottawa sand and Firoozkooh sand used in the past works (Rajabi and Sharifipour 2017b and Rajabi and Sharifipour 2017a) for assessing the effect of hydrocarbon contamination on shear wave velocity.

Table 4.3 Comparison of properties of Guwahati sand and other sands from past literature

Sand Type	**Specific Gravity**	**D_{60}**	**e_{min}**	**e_{max}**
Ottawa sand (Rajabi and Sharifipour, 2017b)	2.65	0.390	0.480	0.780
Firoozkooh sand (Rajabi and Sharifipour, 2017a)	2.63	0.297	0.570	0.845
Guwahati sand (Present Study)	2.62	0.410	0.437	1.06

Subsequent section compares the outcomes of the present study with those obtained through the experimental endeavors conducted by the past researchers to assess the plausible effects of hydrocarbon on the shear wave velocity of sands. Fig. 4.13(a) compares the effect of crude oil content on the S-wave velocity profile reported by Rajabi and Sharifipour (2017b). When compared to the present study both the profiles exhibit single-peaked nature. A fair agreement was observed between the trends of the velocity profiles of published work and the present study. Similar agreement was observed with the past reported results for assessing the effect of confining pressure on shear wave velocity as depicted in Fig. 4.13(b). However, there is a slight variation in the transition points of the two types of sand used in the studies. This variation can be owed to the difference in their respective gradation characteristics.

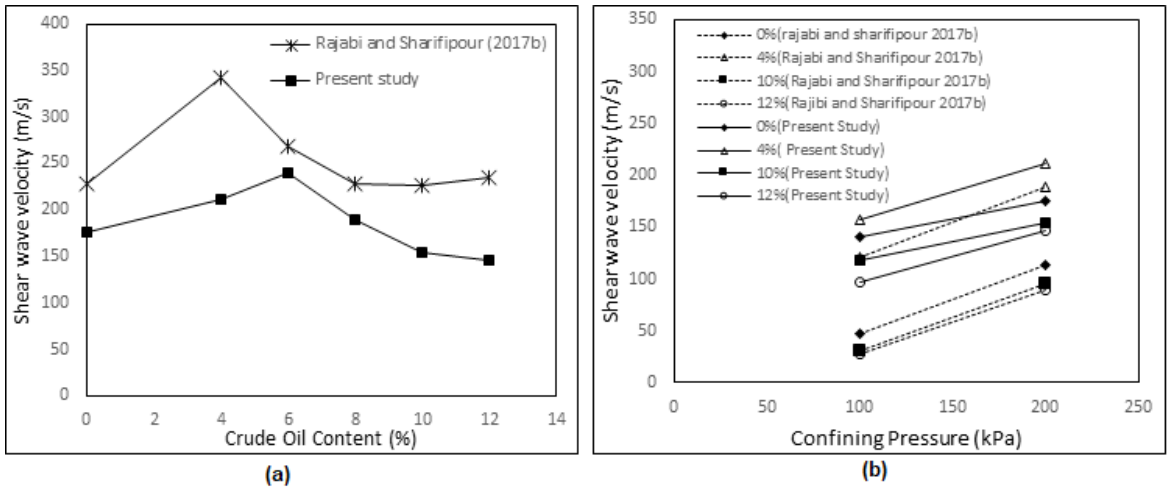

Fig. 4.13 Comparison with past reported results for (a) S-wave velocity versus crude oil content and (b) S- wave velocity versus confining pressure

As discussed previously, the reason behind the initial increase in V_s was the attainment of a more connected structure due to presence of oil droplets on the surface of sand grains. On the other hand, the sharp drop in Vs after transition point was due to total loss of grain to grain contact due to formation oil layer. Comparing the D_{50} and C_u values, which were reported to be 0.35mm and 1.763 respectively for Ottawa sand while 0.25mm and 26.56 respectively for Guwahati sand, it was apparent that the Guwahati sand was finer and relatively well graded as compared to the Ottawa sand. Subsequently, Guwahati sand being well graded requires higher percentage of oil content to smear off the grain to grain contact. In addition, finer sand having higher void ratio may have greater scope to retain oil in its void.

Small strain shear modulus of soil is also an influential parameter in geotechnical applications. It can be easily calculated through bender element test using $G_{max} = \rho V_s^2$. The effect of hydrocarbon contamination on the maximum small strain shear modulus of the sands has been depicted in the Fig. 4.14.

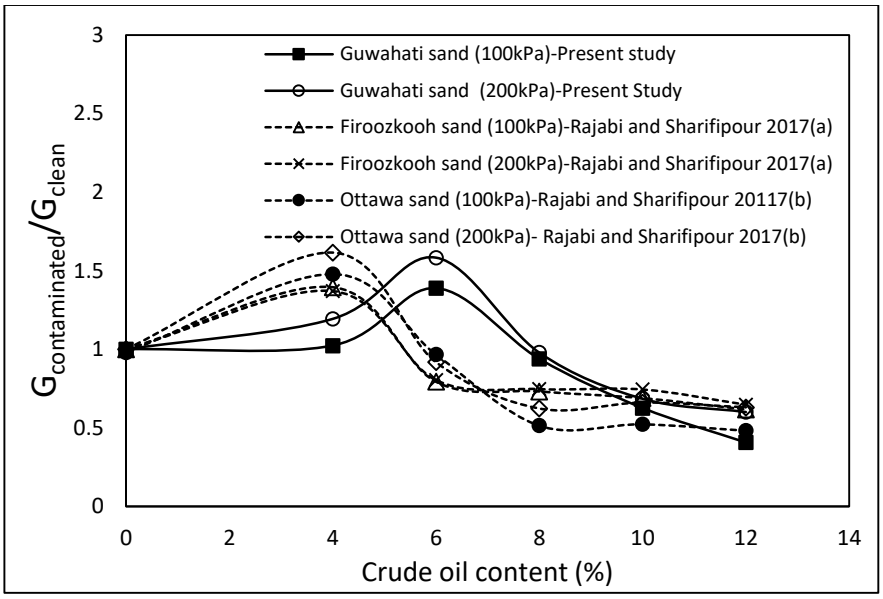

Fig. 4.14 Influence of hydrocarbon contamination on small strain shear modulus of sand

$G_{max,\ cont}$ of the contaminated sands have been normalized considering $G_{max,clean}$ of the clean sand as the base value. According to past results, the effect of crude oil on $G_{max,cont}$ was insignificant after 8%. Notwithstanding, there was a sharp degradation in the $G_{max,cont}$ of Guwahati sand even after 8%.

4.4.5 Effect of Crude Oil Content on Layered Samples

To study the effect of depth of contaminated layer, a series of tests were performed at varying contamination depth ratio (β) considering different oil contents. The influence of varying the contamination depth ratio on the shear wave velocity of the layered specimens has been illustrated in Fig. 4.15 and Fig.4.16 for dry and saturated states respectively at 200 kPa confining stress. The ratio β was varied from 0 to 1 where β=0 denotes the uncontaminated samples while β=1 denotes homogeneously contaminated samples. It can be clearly observed that unlike in saturated samples, the shear wave velocity in dry samples changes linearly with the thickness of the contaminated-sand layer. In case of saturated samples this change was

non-linear where a sharp increase in shear wave velocity was observed initially upto β = 0.6. Further at higher confinement i.e. at 200 kPa, the change was not significant while at lower confining stress, a dip in V_s was observed with increasing β.

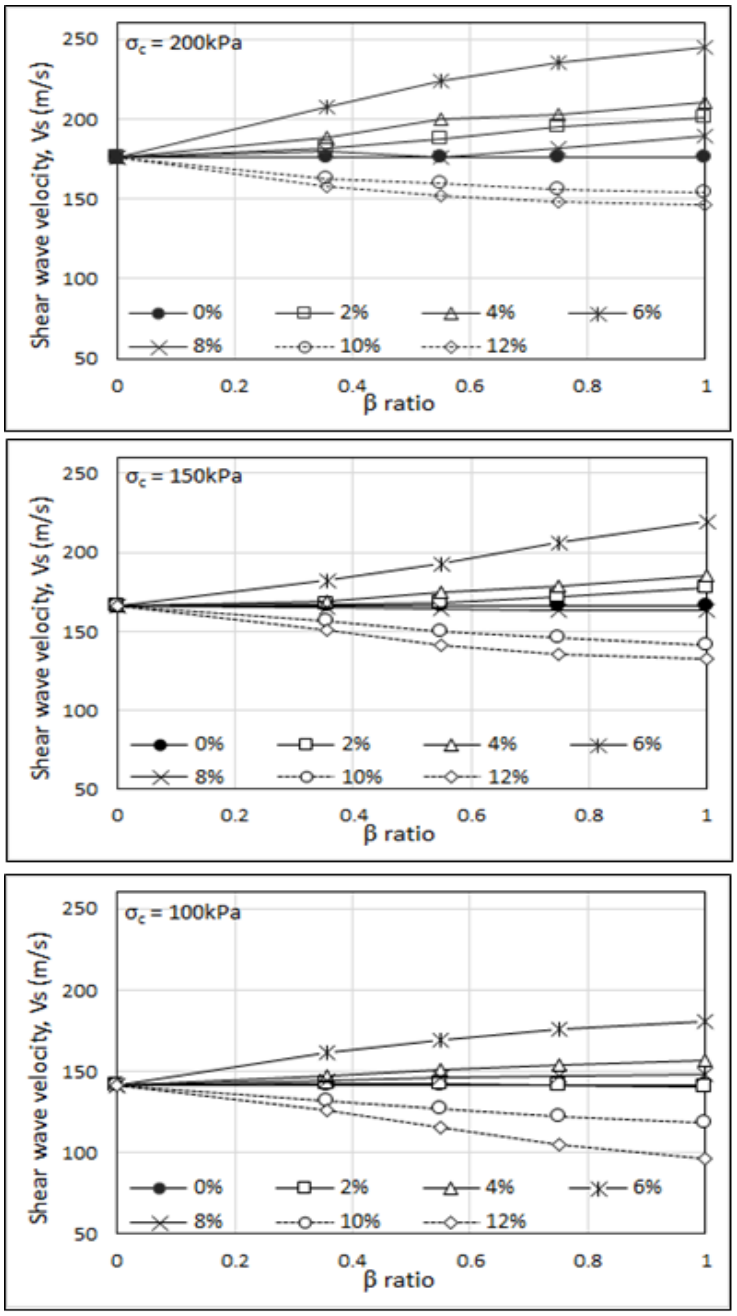

Fig. 4.15 Effect of contaminated-sand layer thickness on shear wave velocity for dry specimens

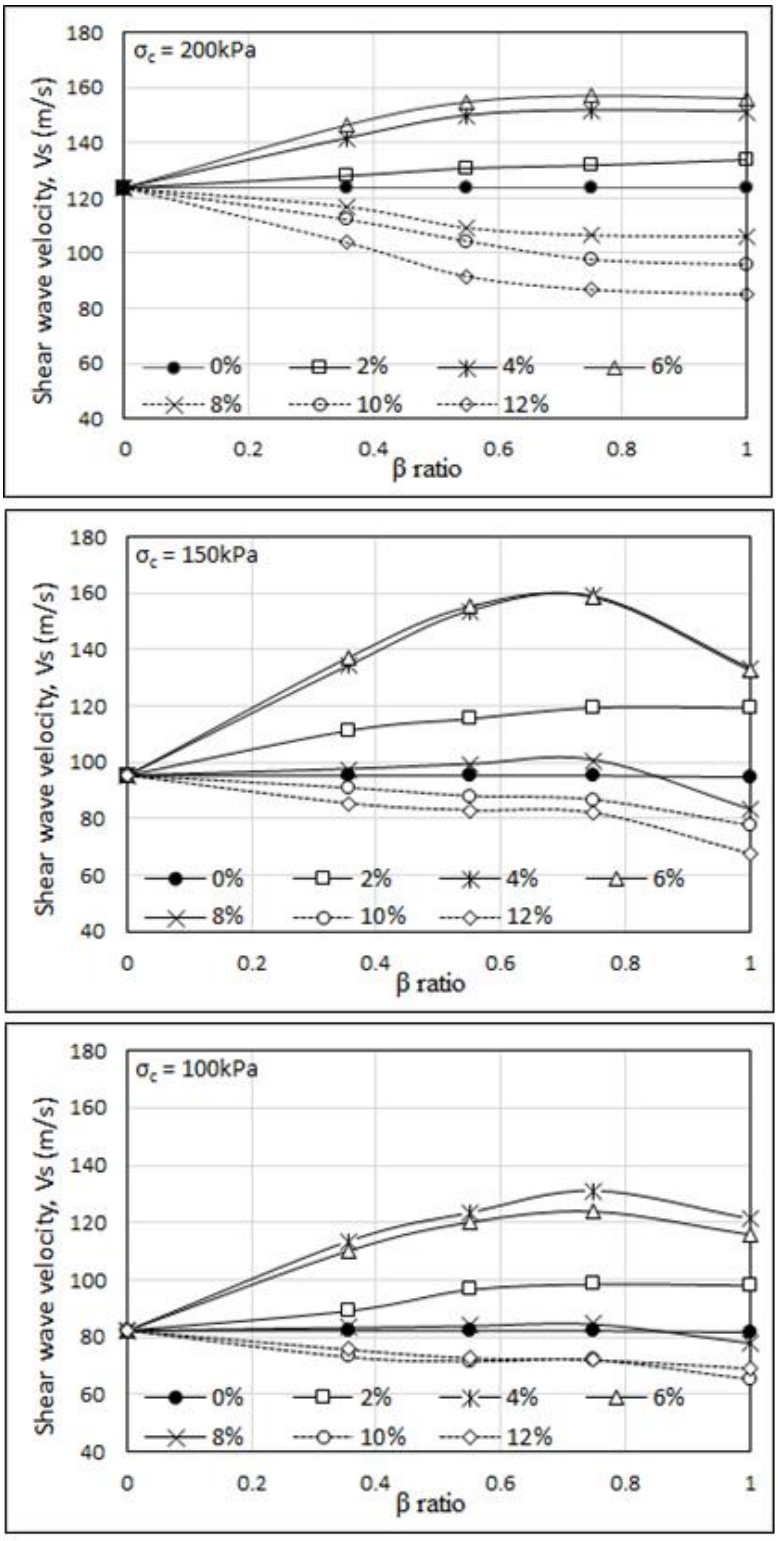

Fig. 4.16 Effect of contaminated-sand layer thickness on shear wave velocity for saturated specimens

4.4.6 Coupled effect of crude oil content and contamination depth ratio

Fig. 4.17 shows the coupled effect of crude oil content and contamination depth ratio on the shear wave velocity of layered soil under confining stresses of 100, 150 and 200 kPa for dry and saturated conditions. In general, the effect of crude oil content on layered sand specimens can be easily correlated with its effect on homogeneously contaminated sand samples. In this regard, from the results explained in earlier sections, it was apparent that the crude oil contamination initially had positive influences on the shear wave velocity. On the other hand, after the transition point it showed diminishing effects. Similarly, for a given β in layered samples, the shear wave velocity tends to increase with increasing crude oil content till the transition point is reached. Adding further crude oil brings substantial negative impact on V_s. However, a remarkable damping was observed in the peaks of the shear wave velocity profiles with decreasing contamination depth ratio. It means the magnitude of peak velocities decreases with decreasing β ratio. It is worth noticing that for each case there exists a point (9.35% for dry samples and 8% for saturated samples) at which the shear wave velocities of contaminated samples were almost unchanged with respect of clean sand at all confining pressures. It may be inferred here that at this point the increase in inter-particle cohesion and decrease in inter-particle friction results in unchanged shear wave velocity. Immediately after the "zero change point" the trend of the change in shear wave velocity with β ratio gets reversed. For highest value β, lowest shear wave velocity was observed. This variation was more pronounced in dry samples.

The significance of zero change point can be understood in such a way that for soil and contaminant specific conditions, the deteriorating effects of hydrocarbon contamination in regard with small-strain problems and liquefaction manifestations starts beyond this point

irrespective of the depth of contamination. However, shear wave velocity cannot be the sole parameter for making such conclusions with strong reliability and hence such an observation requires further experimental verifications through cyclic triaxial and other similar tests.

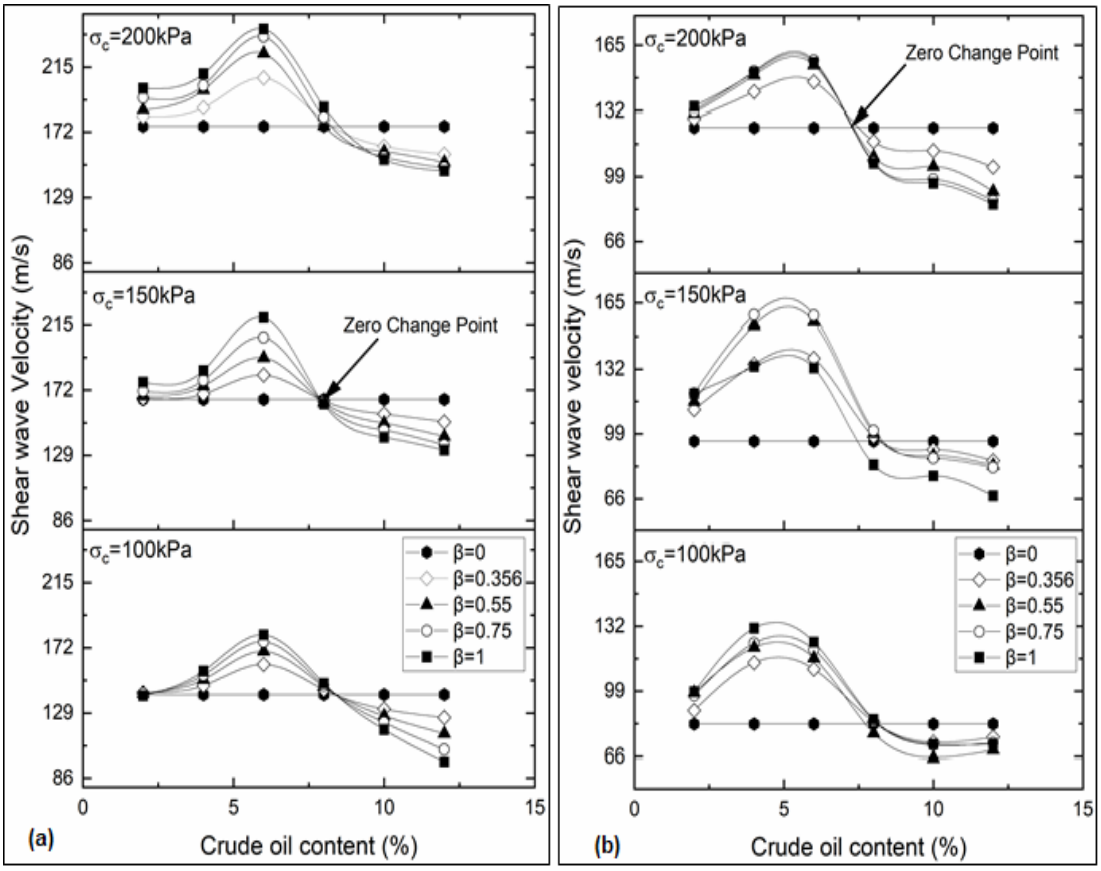

Fig. 4.17 Shear wave velocity profiles of layered samples for different β ratio at varying crude oil content in (a) dry and (b) saturated

4.5 Summary

The study involves a parametric analysis of shear wave velocity in crude oil contaminated sands. The aim was mainly to assess the effect on oil contamination in homogeneous and layered sand samples through conducting a series of bender element test conducting on varying frequency (1-10 kHz), confining pressure (100, 150 and 200 kPa) crude oil content from 0 to 12% and contamination depth ratio, β.

A consistency range in terms of frequency was established within which the sensitiveness of shear wave velocity towards excitation frequency was marginal. The confinement-induced changes were reduced at higher oil content. The variation of shear wave velocity with crude oil contamination gives a single-peaked curve with the maximum shear wave velocity being observed at 6% and 4% in dry and saturated condition respectively. These oil contents have been refereed as "critical oil content". Beyond these critical points, shear wave velocity experiences a sharp dip. For saturated condition at 200 kPa, $V_{s\text{-}6\%} = 1.32V_{s\text{-}clean}$ and $V_{s\text{-}12\%} = 0.72V_{s\text{-}clean}$. The mechanism responsible for the occurrence of transition point was aided with the microstructural examination. Hence, it can be inferred that the initial contamination with hydrocarbon has positive influence on the shear wave velocity and subsequently on cyclic resistance and stiffness. Further contamination beyond the transition point, brings a sharp decline in the shear wave velocity.

The influence of depth of contamination incorporated in terms of β ratio implies that the change in shear wave velocity after $\beta = 0.6$ was insignificant meaning thereby that after 60% of the total considered layer thickness is contaminated, no substantial change in shear wave velocity will be observed with further increase in the depth of contamination. As a non-destructive test, this observation may prove to be helpful in determining the extent of contamination along the ground depth. A critical oil content was observed irrespective of β at which the peak shear wave velocity was observed. However, with increasing β, this peak seems to get suppressed. It is worth mentioning that $V_{s\text{-}9.35\%} \approx V_{s\text{-}clean}$ and hence this point has been termed as "zero change point". At this point, the positive influences of oil contamination get counter-balanced by the negative influences and hence there is no net change in shear wave velocity of oil contaminated sands when compared to clean sand.